ARTICLE

Solvent Effect on the Photoinduced Electron Transfer Reaction Between Thioxanthen-9-one and Diphenylamine†

Lin Chen, Qiao-hui Zhou, Xiang Liu, Xiao-guo Zhou*, Shi-lin Liu

Hefei National Laboratory for Physical Sciences at the Microscale and Department of Chemical Physics, University of Science and Technology of China, Hefei 230026, China

(Dated: Received on March 30, 2015; Accepted on May 24, 2015)

Photoinduced chemical reaction between thioxanthen-9-one (TX) and diphenylamine (DPA) were investigated by the nanosecond laser flash photolysis. With photolysis at 355 nm, the triplet TX (^{3}TX*) is produced via a Franck-Condon excitation and intersystem crossing. In the transient absorption spectra of the reduction of ^{3}TX* by DPA in pure and aqueous CH_3CN, four bands are clearly observed and assigned to absorption of ^{3}TX*, TXH$^\cdot$, TX$^{\cdot-}$ and DPA$^{\cdot+}$, respectively. With the increase of solvent polarity, the blue-shift was observed for all absorption bands of the intermediates. With the aid of dynamic decay curves, an electron transfer followed by a protonation process is confirmed for the reduction of ^{3}TX* by DPA. The quenching rate constants of ^{3}TX* by DPA very slightly decrease from 9.7×10^9 L/(mol·s) in pure CH_3CN, to 8.7×10^9 L/(mol·s) in CH_3CN:H_2O (9:1), 8.0×10^9 L/(mol·s) in CH_3CN:H_2O (4:1) and 7.5×10^9 L/(mol·s) in CH_3CN:H_2O (1:1). Therefore water plays a minor role in the title reaction, and moreover no obvious medium effect of solvent polarity is observed for the electron transfer between ^{3}TX* and DPA, indicating that the $^3n\pi^*$ and $^3\pi\pi^*$ states of TX have the approximate ability to attract an electron from DPA.

Key words: Electron transfer, Protonation, Reaction mechanism, Absorption spectra, Laser flash photolysis

I. INTRODUCTION

Many aromatic ketones, like thioxanthones [1−3] benzophenone (BP) [4, 5], and benzyles [6, 7], have drawn extensive attention of many experiments and theoretical calculations [8−13], due to their important roles in photochemistry and photobiology. In the presence of an electron donor like amines, reductions of the excited electronic state of a ketone are able to form some key radicals in polymer chain reactions, *e.g.* photoreaction of thioxanthone with indolic and phenolic derivatives [14, 15], photoreduction of BP by amines [16−18], and so on. Among all aromatic ketones, thioxanthones are usually used as photoinitiators for dentistry resins [19−21], UV curing of coatings [22], and photopolymerization of monomers in micelles [23]. It is noteworthy that thioxanthone does not directly dissociate to free radicals on UV photolysis, but they can absorb a UV photon to yield the triplet excited state with a high yields [9].

As an important aromatic ketone, thioxanthen-9-one (TX) has a typical conjugated carbonyl structure as shown in Scheme 1, and the ketonic oxygen has a strong ability to attract electron from surroundings (E_{red}=−1.66 eV) [1]. By measuring the nanosecond transient photoconductivity of TX and amino-alkyl radical of triethylamine (TEA-H), Dossot *et al.* observed the thermal electron transfer between the ground state TX and TEA-H$^\cdot$ radical, followed by a fast deprotonation to produce TEA-H$^{\cdot+}$ and TX$^{\cdot-}$ radical ions [25]. Compared with the ground state of TX, the triplet TX is more active to react with electron donors. Yip *et al.* measured the lifetime of ^{3}TX* in different solvents, where the sulfur atom was proposed as the electron donor of charge-transfer complex formed in self-quenching of ^{3}TX* [26]. In the transient absorption spectra of TX in acetonitrile, both the bands at 300 and 600 nm were attributed to ^{3}TX* [27]. By comparing the spectra in different solvents, Ferreira *et al.* found that the maximum absorption of ^{3}TX* has a blue-shift with the polarity of the medium increasing [27]. The recent theoretical calculations [28, 29] indicated that the lowest triplet and singlet excited states of TX are close in energy, so that internal conversion (IC) and intersystem crossing (ISC) are facilitated once photoexcitation and moreover both IC and ISC decrease with the increase of solvent polarity.

In general, the quenching of the triplet thioxanthone

†Dedicated to Professor Qing-shi Zhu on the occasion of his 70th birthday.

*Author to whom correspondence should be addressed. E-mail: xzhou@ustc.edu.cn

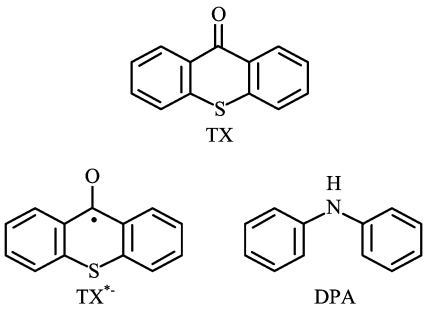

Scheme 1 Molecular structures of TX, $TX^{\cdot-}$, and DPA.

and derivatives by amines is believed to occur via the intermolecular electron transfer mechanism. Therefore, the reduction of $^3TX^*$ by amines is thought as a typical example of the electron transfer, and many investigations has been performed on these photochemical reactions [1, 23, 24, 30−35]. A transient photocurrent measurement [31] on reduction of $^3TX^*$ by two typical amines, 1,4-diazabicyclo[2,2,2]octane (DABCO) and diphenylamine (DPA), were performed respectively. Although the electron transfer from DABCO to $^3TX^*$ was verified, the reduction mechanism between DPA and $^3TX^*$ was uncertain due to too low yield of free ions. Recently, the electron transfers between $^3TX^*$ and triphenylamine (TPA), 3,5,*N*,*N*-tetramethylaniline (TMA) were certified by observing absorptions of $TPA^{\cdot+}$, $TMA^{\cdot+}$ radical cations [35]. In the transient absorption spectra of TX and DPA [24], three new bands in acetonitrile were arbitrarily stated for $TXH^{\cdot}$ (420 nm), $TX^{\cdot-}$ (680 nm), and $DPA^{\cdot+}$ (720 nm), respectively, although the bands were seriously blurred with too low signal-to-noise ratio. It is noteworthy that the spectral assignment of $DPA^{\cdot+}$ radical cation in the experiment is doubtable, because a few previous experiments have the inconsistent conclusions, *e.g.* at 670 nm in methanol [36], at ∼690 nm in low-temperature matrix irradiation experiments [37, 38] and in radiolysis measurement [39]. More significantly, the intensities of the bands at 680 nm ($TX^{\cdot-}$) and 720 nm ($DPA^{\cdot+}$) were not increased simultaneously, which was contradictory with the primary electron-transfer process between $^3TX^*$ and DPA [24]. To verify the electron transfer mechanism it is very necessary to find a confessed spectral assignment of $DPA^{\cdot+}$ radical ion.

It is well known that the triplet excited state of aromatic ketones is formed by promotion of an electron from a nonbonding (n) orbital of oxygen onto an antibonding π^* orbital (noted as $n\pi^*$ configuration). But in a more polar solvent, $^3\pi\pi^*$ state is stabilized as the lowest-lying triplet state [40, 41]. In this case, the primary process of the triplet aromatic ketone in $^3\pi\pi^*$ state usually is a H-abstraction from an environment (R-H) to produce a ketyl radical instead of the electron-transfer, and its rate depends on the ISC yield and its energy [42, 43]. Thus it is worth to reinvestigate the reduction of $^3TX^*$ by DPA in different solvents, to identify that the dominant primary reaction is the electron transfer or H-abstraction process in different polar solvents. Furthermore, to compare the reaction rates in proton inert solvent with the aqueous solvents, it will be very useful to understand the role of water in the title reaction.

In the present experiment, the transient absorption spectra of TX in CH_3CN and CH_3CN:H_2O at different volume ratios with photolysis at 355 nm are measured respectively. With the aid of the quenching dynamics, the new spectral assignments for all intermediates in the reduction of $^3TX^*$ by DPA are obtained, like $TX^{\cdot-}$, $DPA^{\cdot+}$, and $TXH^{\cdot}$ radical. Therefore the whole reduction mechanism of $^3TX^*$ by DPA will be clearly proposed. Moreover, the quenching rate constant of $^3TX^*$ by DPA in various solvents will be derived from the fitting of the quenching rates *vs.* concentration of DPA. The influence of the distributions of $^3\pi\pi^*$ and $n\pi^*$ configurations in $^3TX^*$ on the bimolecular reaction rate constant with DPA will be discussed subsequently.

II. EXPERIMENTS

Steady-state absorption spectra (UV-3600, Shimadzu) and fluorescence spectra (F-4600, Hitachi) of aromatic ketone in different solvents were measured by using commercial spectrometers. The nanosecond laser flash photolysis was performed with a home-made experimental system [44, 45]. A 500 W Xenon lamp was employed as the analyzing sources, and the pulsed photoexcitation source was the third harmonic laser (355 nm, pulse width 8 ns) from an Nd:YAG laser (PRO190, Spectra Physics). The typical power of the pulsed laser is 4 mJ/pulse. Two light beams perpendicularly passed through a flow quartz cuvette with an optical path length of 10 mm. A photomultiplier (CR131, Hamamatsu) was installed at the exit of monochromator to measure intensity of the transmission light. The wavelength range of the spectrometry is 250−800 nm. At a spectral wavelength, the decay curve of intermediate was averaged by multi-shots and recorded with an oscilloscope (TDS3052B, Tektronix). The transient absorption spectra were scanned with an accumulation by 64 shots for each wavelength.

TX (98%), DPA (99%), and TPA (99%) were purchased from Alfa Aesar Co. and Acros Co. respectively, and used without further purification. According to too low solubility of TX and DPA in water, the mixed solvents of acetonitrile and water in different volume ratio are used in the following experiments. Acetonitrile of high performance liquid chromatography reagent and triply-distilled deionized water were used to prepare the aqueous acetonitrile solvent in different ratio. All the solutions were deoxygenated by purging with high-purity argon (99.99%) for 30 min before the spectroscopic and dynamic measurements. The laser

DOI:10.1063/1674-0068/28/cjcp1503054

flash photolysis experiments were performed at ambient room temperature (∼25 °C). In all the following spectral measurements, the concentration of TX was kept as 0.5 mmol/L.

III. RESULTS AND DISCUSSION

It is well-known that both absorption and fluorescence spectra of aromatic ketone can be changed by solvent polarity. With the ratio of water in acetonitrile increasing, solvent polarities are monotonically increasing.

A. Steady-state absorption and fluorescence spectra of TX

The steady-state absorption spectra of TX in different solvents are shown in Fig.1(a), while Fig.1(b) displays their fluorescence spectra under 355 nm irradiation. Only a little red-shift of less than 3 nm is found for the maximum absorption of TX in aqueous acetonitrile compared to that in pure CH_3CN, and absorption intensity is almost unchanged. However the maximum absorption wavelength is red-shifted as the arrow shown in Fig.1(a) with solvent polarity increasing. The fluorescence intensities are dramatically improved with the increasing of solvent polarity, and more than 15 nm red-shift is observed for the maximum fluorescence.

As suggested by Ferreira *et al.* both $^1n\pi^*$ and $^1\pi\pi^*$ characters are involved in the $S_0 \rightarrow S_1$ transition of TX [27]. Although solvent polarity can probably influence energies of $^1n\pi^*$ and $^1\pi\pi^*$ states [40, 41], the Frank-Condon excitation is almost unchanged as shown in Fig.1(a). However with the increase of solvent polarity, $^1\pi\pi^*$ state is significantly stabilized as the lowest singlet excited state [29]. Thus the contribution from $^1\pi\pi^*$ state is enhanced in Fig.1(a), whilst the maximum absorption and fluorescence are red-shift. Moreover, due to decrease in interval conversion (IC) and intersystem crossing (ISC) with the solvent polarity increasing [29], the fluorescence intensity is significantly improved. All the conclusions agree with the most recent calculation [29].

B. Transient absorption spectra of TX in different solvents

Since acetonitrile is inert in chemical reaction, the absorption spectra and dynamic behaviors of TX in pure CH_3CN on photolysis are the simplest and useful to understand its photophysical and photochemical characteristics. The transient absorption spectra of TX in CH_3CN after laser photolysis are shown in Fig.2(a), where four delay times are listed as 0.4, 1.0, 4.2, and 8.6 μs. In the spectra an unique wide peak is observed

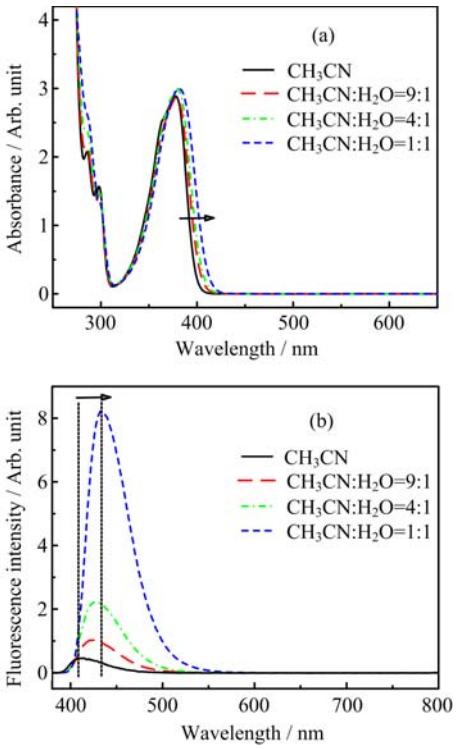

FIG. 1 (a) Steady-state absorption and (b) laser induced fluorescence spectra of TX in different solvents. The arrows show the maximum absorption wavelength and the maximum fluorescence wavelength are red-shifted with solvent polarity increasing.

at 627 nm. It can be attributed to the triplet-triplet transition of $^3TX^*$, as the same as the previous conclusions [24, 27, 35]. Moreover, the assignment is also verified by an additional experiment, in which its intensity was dramatically quenched by the solvated oxygen.

The dynamic decay curves of the intermediate at 627 nm were measured, and the quenching rate k_{obs} of the intermediate was derived from the least square fitting of the curve with a pseudo first-order kinetic. As shown in Fig.2(b), the rates are monotonously increased and the self-quenching rate constant k_{sq} is determined as 9.9×10^8 L/(mol·s), which is far lower than the diffusion-controlling rate limit in acetonitrile (1.94×10^{10} L/(mol·s)). Thus a dynamic excimer is expected to stabilize triplet TX and reduce its self-quenching rate.

Similarly, the transient absorption spectra of TX in CH_3CN:H_2O (9:1), CH_3CN:H_2O (4:1), and CH_3CN:H_2O (1:1) solvents are shown in Fig.3, respectively. With the ratio of water increasing, the absorption intensity of $^3TX^*$ is slightly decreased. The absorption of triplet TX is slightly blue-shifted from 614 nm in CH_3CN:H_2O (9:1), 607 nm in CH_3CN:H_2O (4:1) to 600 nm in CH_3CN:H_2O (1:1). As shown in the most recent calculation [29], the triplet-triplet transition energy of $^3\pi\pi^*$ increases with the increasing of solvent

DOI:10.1063/1674-0068/28/cjcp1503054

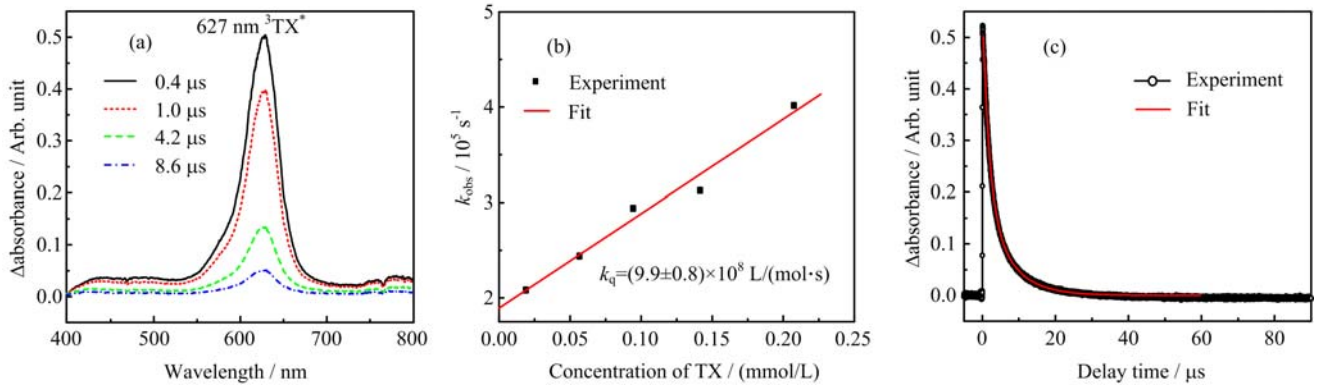

FIG. 2 (a) Transient absorption spectra of TX (0.5 mmol/L) in pure acetonitrile, (b) quenching rate k_{obs} *vs.* concentration of TX, and (c) the experimental and fitted dynamic decay curves of the intermediate at 627 nm.

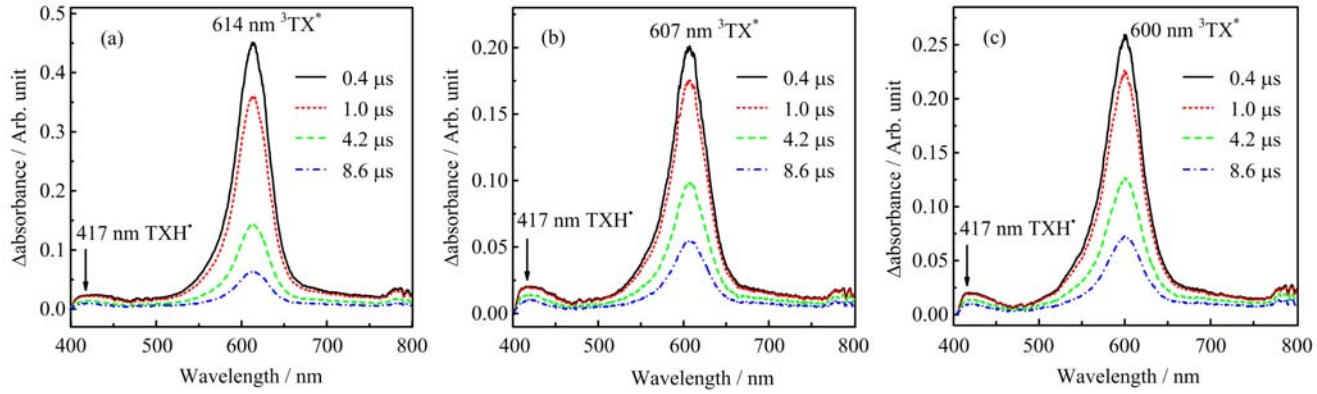

FIG. 3 Transient absorption spectra of TX (0.5 mmol/L) in different aqueous solvents, (a) CH_3CN:H_2O=9:1, (b) CH_3CN:H_2O=4:1, and (c) CH_3CN:H_2O=1:1.

polarity. It is consistent with the present phenomenon of blue-shift. In addition, interval conversion (IC) and intersystem crossing (ISC) are weakened with the solvent polarity increasing [29], and hence the absorption intensity of ^{3}TX* is certainly decreased.

By fitting the decay of absorption intensity of ^{3}TX*, its quenching rates are measured and summarized in Table I. Due to hydrogen bond between hydroxyl of water and keto oxygen of TX, the direct H-abstraction easily occurs in a protic solvent. Thus a new weak absorption at ∼417 nm in Fig.3 can be assigned as the absorption of TXH$^·$ radical according to the previous conclusions [24, 27, 35]. Moreover, no electron transfer does evidently occur in these solutions because no absorption of TX$^{·-}$ radical anion is observed at ∼680 nm. Thus the overall quenching mechanism of ^{3}TX* in a protic solvent is a competition between the self-quenching and the H-abstraction processes. As shown in Table I, the quenching rate of ^{3}TX* is decreased with a sequence of CH_3CN:H_2O (9:1, 4:1, and 1:1) solvents. It is well consistent with the fact that the $^3\pi\pi^*$ state is less reactive towards H-abstraction [46]. The greater the polarity of the solvent is, the more dominant the $^3\pi\pi^*$ state of ^{3}TX* is, and hence the quenching rate the slower is.

C. Photo-induced chemical reaction between TX and DPA in pure acetonitrile

In the presence of DPA, transient absorption spectrum of TX in pure acetonitrile was measured and shown in Fig.4. Intensity of the absorption at 627 nm is dramatically reduced from that in Fig.2(a), while that at 420 nm is notably improved. Two new absorptions at ∼683 and 780 nm can also be clearly observed with the weak intensities, especially at the delay time of 1.0 μs.

The dynamic decay of these four absorptions was measured and shown in Fig.5(a). It is similar to Fig.2(a) that the bands at 627 and 420 nm can be assigned to the absorptions of ^{3}TX* (627 nm) and TXH$^·$ radical (420 nm), respectively. Obviously, the decay rate of ^{3}TX* is much faster than that in the absence of DPA, indicating that a fast reaction between ^{3}TX* and DPA definitely happens. With the quenching of ^{3}TX*, the intermediates at 683 and 780 nm are produced quickly with a close rate. Both the absorptions reach the maximum at about 0.7 μs and then decrease. Thus both the intermediates should be the initial reaction products of ^{3}TX* and DPA. Moreover, the absorption at 420 nm is gradually increased to its maximum at about 1.2 μs,

DOI:10.1063/1674-0068/28/cjcp1503054

TABLE I Absorption wavelengths λ, lifetime t, and quenching rates k_{obs} of intermediates after photolysis of TX (0.5 mmol/L) in different solvents.

CH_3CN:H_2O	$TXH^{\cdot}$			$^3TX^*$		
	t/μs	$k_{obs}/10^5$ s^{-1}	λ/nm	t/μs	$k_{obs}/10^5$ s^{-1}	λ/nm
1:0	–	–	–	1.98±0.02	5.05±0.04	627
9:1	4.73±0.06	2.11±0.03	417	2.32±0.03	4.30±0.06	614
4:1	4.85±0.05	2.06±0.02	417	2.90±0.07	3.45±0.08	607
1:1	5.15±0.09	1.94±0.04	417	3.85±0.09	2.60±0.06	600

TABLE II Lifetime t, quenching rate k_{obs}, and absorption wavelength λ of all intermediates[a].

	CH_3CN:H_2O	λ/nm	$k_{obs}/10^5$ s^{-1}	t/μs		CH_3CN:H_2O	λ/nm	$k_{obs}/10^5$ s^{-1}	t/μs
$TXH^{\cdot}$	1:0	420	1.85±0.03	5.39±0.07	$^3TX^*$	1:0	627	27.21±0.04	0.3675±0.0005
	9:1	418	1.80±0.03	5.55±0.07		9:1	614	27.17±0.05	0.3680±0.0006
	4:1	418	1.75±0.03	5.71±0.07		4:1	607	25.72±0.04	0.3887±0.0006
	1:1	418	1.62±0.03	6.17±0.09		1:1	600	23.35±0.05	0.4282±0.0008
$TX^{\cdot-}$	1:0	683	3.44±0.04	2.90±0.03	$DPA^{\cdot+}$	1:0	780	2.04±0.09	4.9±0.2
	9:1	683	3.74±0.05	2.67±0.03		9:1	780	2.00±0.09	5.0±0.2
	4:1	683	3.42±0.05	2.92±0.04		4:1	780	2.00±0.05	5.0±0.1
	1:1	683	2.63±0.04	3.79±0.05		1:1	780	1.72±0.06	5.8±0.2

[a] Concentration of DPA is 3 mmol/L.

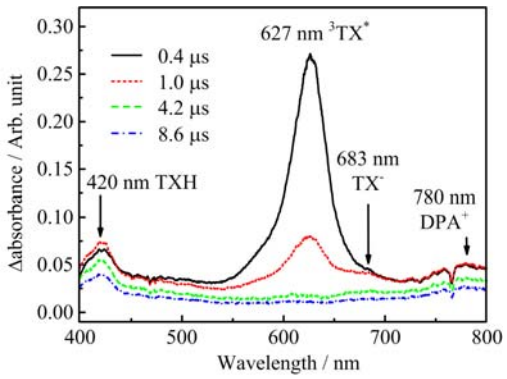

FIG. 4 Transient absorption spectra of TX and DPA in pure CH_3CN at different time delay after photolysis.

and hence it is naturally attributed to a product of the secondary reaction.

By using the least square fitting with the first-order or second-order kinetics, the quenching rates of the intermediates are obtained and summarized in Table II. It is well known that DPA has a low oxidation potential as a common electron donor in reaction, so that it can provide an electron to $^3TX^*$. Thus $DPA^{\cdot+}$ and $TX^{\cdot-}$ radical ions are expected via an initial electron transfer process of Eq.(1). Thus the spectral carriers of the absorptions at 780 and 683 nm are straightly assigned to the products of the electron-transfer process, $DPA^{\cdot+}$ and $TX^{\cdot-}$ radical ions. Since there are the inconsistent spectral assignments of the absorptions of $DPA^{\cdot+}$ radical cation, an additional experiment on photoreaction between TX and TPA was done in order to clarify the absorption of $DPA^{\cdot+}$ in CH_3CN. Due to the lower oxidation potential of TPA than that of DPA, the electron transfer is primary between $^3TX^*$ and TPA. Figure 6 shows the transient absorption spectra with photolysis at 355 nm, where several absorptions are visible at 420, 550, 627, and 670 nm. It is well-known that absorption of $TPA^{\cdot+}$ has the maximum at ∼550 nm in acetonitrile [47], the peak at 670 nm is certainly assigned to the contribution of $TX^{\cdot-}$ radical anion. By comparing the spectra in Fig.4 with that in Fig.6, the spectral carrier of the weak absorption at 780 nm in Fig.4 is believed to be contributed by $DPA^{\cdot+}$ radical cation. It is noteworthy that the weak absorption of $DPA^{\cdot+}$ in CH_3CN covers such a wide wavelength range that it is difficult to identify the peak position. It is believed as the chief reason to cause the inconsistence in all the references.

Once producing, $TX^{\cdot-}$ radical anion can rapidly abstract a proton from $DPA^{\cdot+}$ to produce $TXH^{\cdot}$ radical as Eq.(2). $TXH^{\cdot}$ radical contributes to the 420 nm band as the same as Fig.3. The quenching rates of $TX^{\cdot-}$ and $DPA^{\cdot+}$ are close indeed as shown in Table II, and the slight faster rate of $TX^{\cdot-}$ probably is due to contamination of the nearby absorption of $^3TX^*$.

$$^3TX^* + DPA \rightarrow {}^3[TX^- \cdots DPA^+] \rightarrow TX^{\cdot-} + DPA^{\cdot+} \quad (1)$$

$$TX^{\cdot-} + DPA^{\cdot+} \rightarrow TXH^{\cdot} + (DPA_{-H})^{\cdot} \quad (2)$$

As shown in Fig.5(b), the obvious quenching rates k_{obs} monotonically increase with the DPA concentration, and a linear relationship is found. Using fitting with the Stern-Volmer relationship as Eq.(3),

DOI:10.1063/1674-0068/28/cjcp1503054

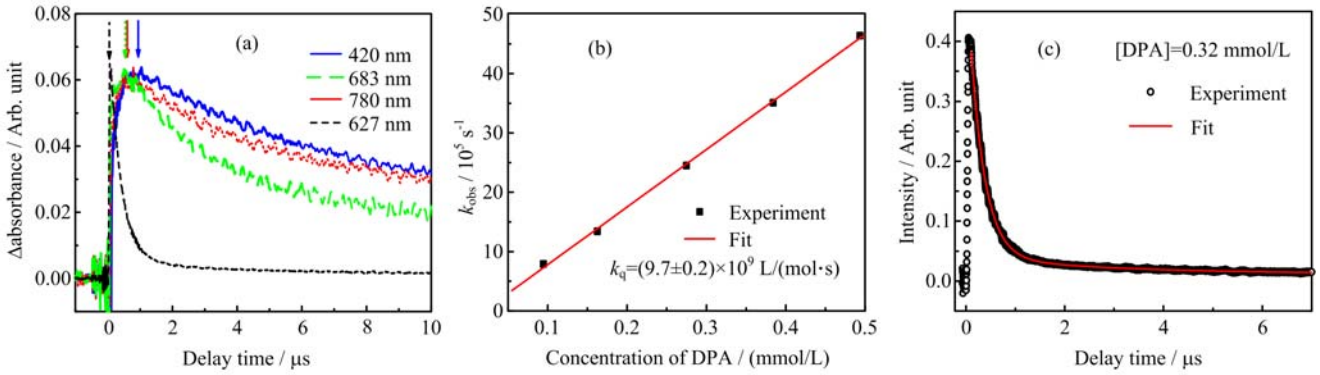

FIG. 5 (a) Normalized dynamic decay curves of the intermediates at 420, 627, 683, and 780 nm in pure acetonitrile, where the arrows show the delay time to reach the maximum of absorption, (b) quenching rate of triplet TX *vs.* concentration of DPA, and (c) the experimental and fitted dynamic decay curves of the intermediate at 627 nm.

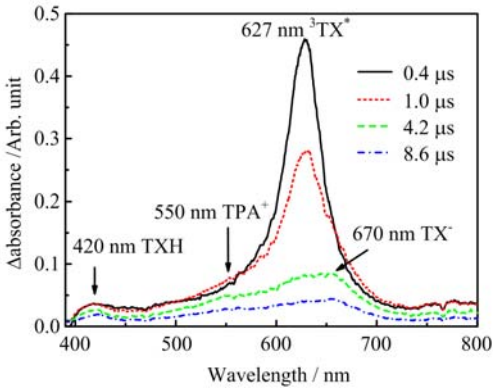

FIG. 6 Transient absorption spectra of TX and TPA in pure CH_3CN at different delay time after photolysis.

the quenching rate constant k_q can be determined as 9.7×10^9 L/(mol·s), which is close to encounter-controlled rate constant in CH_3CN.

$$k_{obs} = k_0 + k_q[DPA] \quad (3)$$

where k_0 and k_{obs} are the quenching rate of ^{3}TX* (0.5 mmol/L) in solution of the absence and presence of DPA, respectively. Obviously, the quenching rate constant k_q is much higher than the self-quenching rate constant k_{sq} (9.9×10^8 L/(mol·s)), and thus the quenching of triplet TX by DPA is very effective indeed.

To confirm the electron transfer mechanism between ^{3}TX* and DPA, the free Gibbs free energy change ΔG is calculated by the Rehm-Weller Eq.(4),

$$\Delta G = E_{ox} - E_{red} - \frac{q^2}{\varepsilon r} - E_T \quad (4)$$

where E_{ox} and E_{red} are the oxidation potential of DPA and the reduction potential of ^{3}TX*, respectively. E_T is the excited energy of the triplet TX, 274.4 kJ/mol [48]. For DPA, the value of E_{ox} is 0.84 eV (*vs.* SCE) in acetonitrile. For ^{3}TX*, the value of E_{red} is −1.66 eV (*vs.* SCE) in acetonitrile. $q^2/\varepsilon r$ is the Coulombic work term of the product ions at the encounter distance, and the value is 0.055 eV in acetonitrile [35]. Thus ΔG of the electron transfer reaction Eq.(1) is determined as −0.4 eV, indicating the electron transfer is able to occur between ^{3}TX* and DPA indeed.

D. Photochemical reaction between TX and DPA in protic solvents

Figure 7 shows the transient absorption spectra of TX and DPA in two protic solvents of CH_3CN:H_2O (9:1 and 1:1). The four bands in Fig.4 are also visible with slight wavelength-shifts. The maximum absorptions at 614 or 600 nm are shifted from 627 nm in pure acetonitrile and still assigned to triplet-triplet absorption of ^{3}TX*. Compared with the spectrum in Fig.4, intensity of triplet TX is reduced at the same delay time. Similarly, the absorptions at ∼418, ∼673, and 780 nm are contributed by $TXH^{\cdot-}$ radical, $TX^{\cdot-}$ radical anion and $DPA^{\cdot+}$ radical cation, respectively, and exhibit slight blue-shift from those in pure CH_3CN. Solvent polarity is believed to be the most significant reason of the blue-shift.

Similar to quenching in pure acetonitrile, the electron transfer between ^{3}TX* and DPA and the protonation process between $TX^{\cdot-}$ and $DPA^{\cdot+}$ radical ions are expected as well in protic solvent. By fitting the decay curves, the quenching rates of the intermediates were obtained and summarized in Table II as well. Obviously, the quenching rates of ^{3}TX* slightly decrease with the increase of water ratio, although an additional reduction pathway of the H-abstraction from H_2O definitely exists. However due to too low rate of H-abstraction process, water are believed to play a minor role in the photoinduced reaction of TX and DPA. Furthermore, in Fig.8 the obtained rates *vs.* the concentration of DPA are plotted. The observed rates monotonically increase with the DPA concentration as a linear relationship. Using fitting with the Stern-Volmer relationship Eq.(3), k_q can be de-

DOI:10.1063/1674-0068/28/cjcp1503054

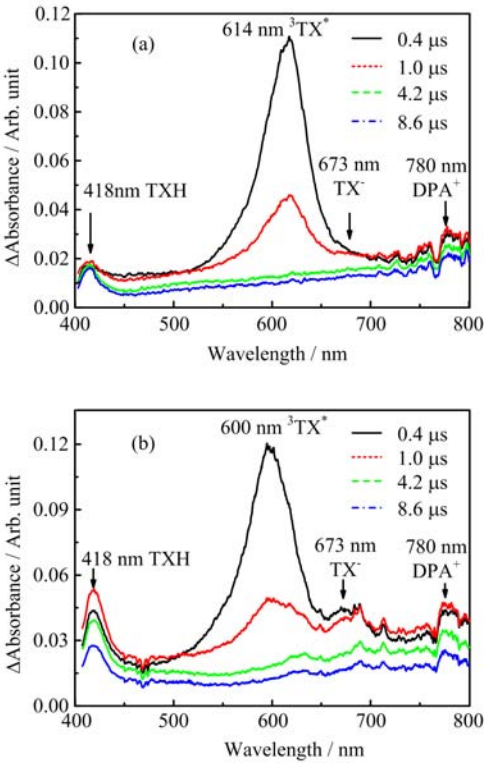

FIG. 7 Transient absorption spectra of TX (0.5 mmol/L) and DPA (0.3 mmol/L) in protic solvents of CH_3CN:H_2O as different ratio of (a) 9:1 and (b) 1:1 with photolysis at 355 nm.

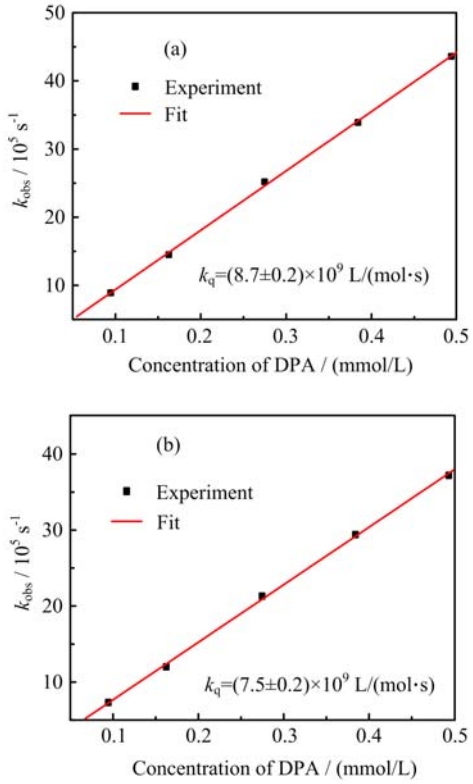

FIG. 8 Dependence of the observed quenching rates of ^{3}TX* on concentration of DPA in (a) CH_3CN:H_2O=9:1 and (b) CH_3CN:H_2O=1:1.

termined as 8.7×10^9 L/(mol·s) (in CH_3CN:H_2O=9:1), 8.0×10^9 L/(mol·s) (in CH_3CN:H_2O=4:1), and 7.5×10^9 L/(mol·s) (in CH_3CN:H_2O=1:1), all of which are close to the encounter-controlled rate constant. Therefore, the dominant quenching process of ^{3}TX* by DPA in protic solvent is still the electron-transfer, which is consistent with the case of pure CH_3CN. The corresponding rate constant slightly decreases with the increase of solvent polarity.

As the recent calculation suggested [29], both $^3n\pi^*$ and $^3\pi\pi^*$ states of TX exist in polar solvent with different population ratio. With the increase of solvent polarity, the $^3\pi\pi^*$ configuration becomes more dominant. However, the decay rates of ^{3}TX* in all media of Table II are approximate. Therefore the $^3n\pi^*$ and $^3\pi\pi^*$ states of TX should have the approximate ability to attract an electron from DPA, although the $^3\pi\pi^*$ state is less reactive towards hydrogen atom abstraction [46].

IV. CONCLUSION

Photoinduced chemical reactions between TX and DPA in pure and aqueous acetonitrile have been investigated by the method of the nanosecond laser flash photolysis. With photolysis at 355 nm, triplet TX (^{3}TX*) is produced via a Franck-Condon excitation and intersystem crossing with a high yield. Without any chemical quenchers, only a wide band at 627 nm is observed in the transition absorption spectra, which is assigned as the triplet-to-triplet transition of ^{3}TX*. In the protic solvents, a weak absorption at 417 nm appears and is attributed by TXH$^\cdot$ radical, which is formed via a direct H-abstraction of ^{3}TX* from water. No electron transfer does evidently occur since no absorption of TX$^{\cdot-}$ radical anion is observed.

In the presence of DPA, reduction of ^{3}TX* occurs via a typical two-step mechanism of the electron transfer and protonation process. The TX$^{\cdot-}$ radical anion and DPA$^{\cdot+}$ radical cation are found to contribute to the bands at 683 and 780 nm, respectively, in pure acetonitrile. Since there are uncertain assignments of DPA$^+$ in the previous experiments, an additional experiment of the electron transfer between ^{3}TX* and TPA has been done. The results indicate that the absorption of DPA$^+$ cation is a really wide and gradual band with a maximum at 780 nm in pure acetonitrile. Thus the absorption at 683 nm is straightly assigned to TX$^{\cdot-}$, which is consistent with the previous conclusions. Following the primary electron-transfer process, a protonation process between TX$^{\cdot-}$ and DPA$^{\cdot+}$ is proposed to form TXH$^\cdot$ radical. Through fitting the decay rate of ^{3}TX* with the concentration of DPA, the quenching rate constant is determined as 9.7×10^9 L/(mol·s) in pure acetonitrile. In the polar

DOI:10.1063/1674-0068/28/cjcp1503054

solvents, the blue-shift was observed for all absorption bands of the intermediates in the title reaction. The quenching rate constants of $^3TX^*$ by DPA are determined as 8.7×10^9 L/(mol·s) (in CH_3CN:H_2O=9:1), 8.0×10^9 L/(mol·s) (in CH_3CN:H_2O=4:1), and 7.5×10^9 L/(mol·s) (in CH_3CN:H_2O=1:1), respectively. Thus the dominant quenching process of $^3TX^*$ by DPA in protic solvent is still the electron-transfer, where water plays a minor role. The corresponding rate constant slightly decreases with the increase of solvent polarity. Therefore no obvious medium effect of solvent polarity is observed for the electron transfer between $^3TX^*$ and DPA, indicating that the $^3n\pi^*$ and $^3\pi\pi^*$ states of TX have the approximate ability to attract an electron from DPA.

V. ACKNOWLEDGMENTS

This work was supported by the National Natural Science Foundation of China (No.21373194) and the National Key Basic Research Special Foundation (No.2013CB834602).

[1] S. F. Yates and G. B. Schuster, J. Org. Chem. **49**, 3349 (1984).
[2] J. P. Fouassier, D. J. Lougnot, I. Zuchowicz, P. N. Green, H. J. Timpe, K. P. Kronfeld, and U. Muller, J. Photochem. **36**, 347 (1987).
[3] D. G. Anderson, R. S. Davidson, and J. J. Elvery, Polymer **37**, 2477 (1996).
[4] L. A. Linden, J. Paczkowski, J. F. Rabek, and A. Wrzyszczynski, Polimery **44**, 161 (1999).
[5] F. Scigalski and J. Paczkowski, Polimery **52**, 19 (2007).
[6] D. J. Lougnot and J. P. Fouassier, J. Polym. Sci. Part A **26**, 1021 (1988).
[7] F. Catalina, C. Peinado, M. Blanco, N. S. Allen, T. Corrales, and I. Lucas, Polymer **39**, 4399 (1998).
[8] F. Morlet-Savary, C. Ley, P. Jacques, F. Wieder, and J. P. Fouassier, J. Photochem. Photobiol. A **126**, 7 (1999).
[9] X. Allonas, C. Ley, C. Bibaut, P. Jacques, and J. P. Fouassier, Chem. Phys. Lett. **322**, 483 (2000).
[10] C. Ley, F. Morlet-Savary, J. P. Fouassier, and P. Jacques, J. Photochem. Photobiol. A **137**, 87 (2000).
[11] L. T. Okano, T. C. Barros, D. T. H. Chou, and A. J. Bennet, J. Phys. Chem. B **105**, 2122 (2001).
[12] H. Satzger, B. Schmidt, C. Root, W. Zinth, B. Fierz, F. Krieger, T. Kiefhaber, and P. Gilch, J. Phys. Chem. A **18**, 10072 (2004).
[13] M. Goez and B. H. M. Hussein, Phys. Chem. Chem. Phys. **6**, 5490 (2004).
[14] D. Das and D. N. Nath, J. Phys. Chem. A **112**, 11619 (2008).
[15] L. Shen and H. F. Ji, Int. J. Mol. Sci. **10**, 4284 (2009).
[16] S. G. Cohen and S. Ojanpera, J. Am. Chem. Soc. **97**, 5633 (1975).
[17] S. Inbar, H. Linschitz, and S. G. Cohen, J. Am. Chem. Soc. **102**, 1419 (1980).
[18] K. S. Peters, E. Pang, and J. Rudzki, J. Am. Chem. Soc. **104**, 5535 (1982).
[19] T. Hayakawa and K. Horie, Dent. Mater. **8**, 351 (1992).
[20] K. Nakanuma, T. Hayakawa, T. Tomita, and Y. Muneyoshi, Dent. Mater. **14**, 281 (1998).
[21] T. Hayakawa, K. Kikutake, and K. Nemoto, Dent. Mater. J. **18**, 324 (1999).
[22] M. J. Davis, J. Doherty, A. A. Godfrey, P. N. Green, J. R. A. Young, and M. A. Parrish, J. Oil Colour Chem. Assoc. **61**, 256 (1978).
[23] J. P. Fouassier and D. J. Lougnot, J. Appl. Polym. Sci. **34**, 477 (1987).
[24] F. Scigalski and J. Paczkowski, Macromol. Chem. Phys. **209**, 1872 (2008).
[25] M. Dossot, X. Allonas, and P. Jacques, Res. Chem. Intermed. **29**, 21 (2003).
[26] R. W. Yip, A. G. Szabo, and P. K. Tolg, J. Am. Chem. Soc. **95**, 4471 (1973).
[27] G. C. Ferreira, C. C. Schmitt, and M. G. Neumann, J. Braz. Chem. Soc. **17**, 905 (2006).
[28] V. Rai-Constapel, S. Salzmann, and C. M. Marian, J. Phys. Chem. A **115**, 8589 (2011).
[29] G. Angulo, J. Grilj, E. Vauthey, l. Serrano-Andres, O. Rubio-Pons, and P. Jacques, Chem. Phys. Chem. **11**, 480 (2010)
[30] S. G. Cohen, A. Parola, and G. H. Parsons, Chem. Rev. **73**, 141 (1973).
[31] Q. Q. Zhu, W. Schnabel, and P. Jacques, J. Chem. Soc. Faraday Trans. **87**, 1531 (1991).
[32] X. S. Jiang and J. Yin, Macromolecules **37**, 7850 (2004).
[33] X. S. Jiang, H. J. Xu, and J. Yin, Polymer **45**, 133 (2004).
[34] X. S. Jiang and J. Yin, Polymer **45**, 5057 (2004).
[35] Q. Sun, J. T. Wang, L. M. Zhang, and M. P. Yang, Acta Phys. Chim. Sin. **26**, 2481 (2010).
[36] R. Rahn, J. Schroeder, J. Troe, and K. H. Grellmann, J. Phys. Chem. **93**, 7841 (1989).
[37] T. Shida, Y. Nosaka, and T. Kato, J. Phys. Chem. **82**, 695 (1978).
[38] G. N. Lewis and D. Lipkin, J. Am. Chem. Soc. **64**, 2801 (1942).
[39] T. Shida and W. H. Hamill, J. Chem. Phys. **44**, 2369 (1966).
[40] J. J. Cavaleri, K. Prater, and R. M. Bowman, Chem. Phys. Lett. **259**, 495 (1996).
[41] M. G. Neumann, M. H. Gehlen, M. V. Encinas, N. S. Allen, T. Corrales, C. Peinado, and F. Catalina, J. Chem. Soc. Fraday Trans. **93**, 1517 (1997).
[42] N. S. Allen, *Photopolymerization and Photoimaging Science and Technology*, New York: Elsevier, (1989).
[43] J. P. Fouassier, *Photoinitiation, Photopolymerization and Photocuring; Fundamentals of Applications*, Munich: Hanser Publishers, (1995).
[44] X. Liu, L. Chen, Q. H. Zhou, X. G. Zhou, and S. L. Liu, J. Photochem. Photobiol. A **269**, 42 (2013).
[45] X. Liu, L. Chen, Q. H. Zhou, X. G. Zhou, and S. L. Liu, Chin. J. Chem. Phys. **26**, 498 (2013).
[46] C. H. Evans, N. Prud'homme, M. King, and J. C. Scaiano, J. Photochem. Photobiol. A **121**, 105 (1999).
[47] R. F. Bartholomew, R. S. Davidson, P. F. Lambeth, J. F. McKellar, and P. H. Turner, J. Chem. Soc. Perkin Trans. **2**, 577 (1972).
[48] W. G. Herkatroeter, A. A. Lamula, and G. S. Hammond, J. Am. Chem. Soc. **86**, 4537 (1964).

DOI:10.1063/1674-0068/28/cjcp1503054